

## MTF characteristics of a Scophony scene projector.

Eric Schildwachter

Martin Marietta  
Electronics, Information & Missiles Systems  
PO Box 555837, Orlando, Florida 32855-5837

Glenn Boreman

University of Central Florida  
CREOL  
Electrical Engineering Dept  
Orlando, Florida 32816

### ABSTRACT

The Scophony Scene Projector has been examined in detail. Modulation Transfer Function was measured and found to be significantly lower than expected. The discrepancy is shown to be due to variation in the Bragg angle with input frequency. Experimental data is compared with calculated performance.

### 1. INTRODUCTION

The IR scene projector is a required tool of today's electro-optical engineer or technician. Testing of sophisticated infrared systems requires acquiring imagery through the system's optics and detector(s) in order to test all aspects of the design and manufacture. Scene generators and projectors allow the images of a test range or mission sequence to be acquired by the sensor under test while never leaving the lab bench or hardware facility. The fidelity of these images must be sufficient to test the MTF of the sensor system. The specific hardware utilized in this experiment was an infrared scene projector on loan to CREOL from the Naval Training Systems Center, Orlando, FL; but the discussion and results are applicable to any wavelength of interest.

### 2. SCANNING SCENE PROJECTORS

In a scanning scene projector the scene is painted onto the image plane using a high intensity light source. A laser is an obvious choice of light source. The image is delivered as the equivalent in-band flux. For example an 8 to 12 micron scene is projected using a CO<sub>2</sub> at 10.6 microns with the same total flux as the original scene. The full dynamic range of the sensor may be tested although the exact spectral characteristics of the system may not. Two distinct laser scanner formats exist: the flying spot scanner and the Scophony scanner. These systems are very similar in hardware configuration but differ in their modulation of the laser beam. Both use an acousto-optic Bragg cell to intensity modulate the laser beam and in both cases the acousto-optic modulator is orientated such that light enters at the Bragg angle. The input video signal is used to amplitude modulate an acousto-optic drive signal which is equal to 40 MHz in this experiment. Light energy will diffract into the first order diffraction lobe proportional to the drive signal amplitude as shown in figure 1 and this beam is scanned horizontally and vertically to generate a 2D image. The Bragg angle,  $\Theta_B$  in air is defined<sup>1</sup> as

$$\sin \Theta_B = \lambda f_a / 2v \quad (1)$$

where  $f_a$  is the acoustic frequency and  $v$  is the acoustic wave velocity. The modulated drive signal is sent to a piezoelectric transducer on the acousto-optic crystal which translates the electrical signal into an acoustic signal within the crystal. The signal traverses the acousto-optic aperture at the speed of sound in the acousto-optic medium and is absorbed in an absorptive material to prevent reflections back toward the transducer. Rise time is equal to the laser beam diameter divided by the acoustic velocity<sup>1</sup>. In a flying spot scanner the laser beam is focussed to a small spot in order to have a fast rise time. This single point of the image is scanned to produce the entire image point by point.

The Scophony technique was developed at the Scophony Laboratories outside of London during the 1930's<sup>2</sup>. Video information is modulated onto the laser beam in an acousto-optic cell just as in a flying spot scanner, however, the Scophony technique uses a collimated laser beam to fill a large portion of the acousto-optic aperture. By spreading the laser beam across the acousto-optic aperture, several "points" of the image are simultaneously modulated. This fan of information

is scanned to form the image with one very important consideration. Since the video information is travelling across the acousto-optic cell, the Scophony technique must utilize the horizontal scan velocity to act as an offsetting motion, thus allowing the video information to remain stationary at the image plane.

The layout for the Scophony process is shown in Figure 2. The information moves across the crystal at the speed of sound in the cell medium (which for this discussion is germanium and the appropriate speed of sound,  $V_{\text{sound}}$ , is 5506.5 meters per second.) Obviously, the information will also be traveling across the light beam with the same velocity. The information must be stationary in the image plane in order to view the scene. This is accomplished by appropriately balancing the optics and the scan velocity. The lenses focus the beam onto a mirror of a polygon scanner acting as the horizontal scanner located at the deflector plane in the figure. The magnification,  $M$ , will scale the information motion to  $MV_{\text{sound}}$ . The scanner will also impart an additional velocity on the beam,  $V_{\text{scan}}$ .

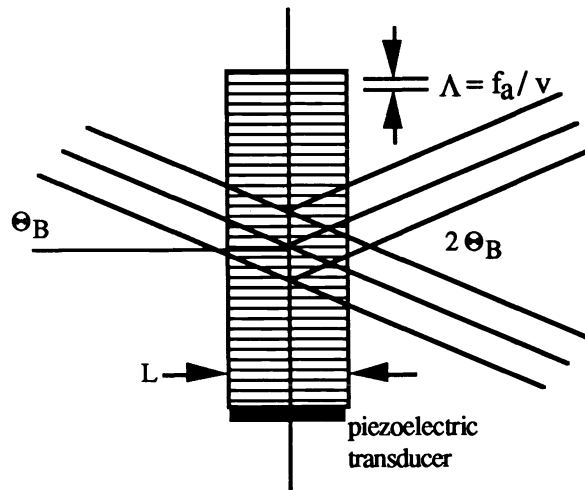


Figure 1. Bragg Angle Geometry

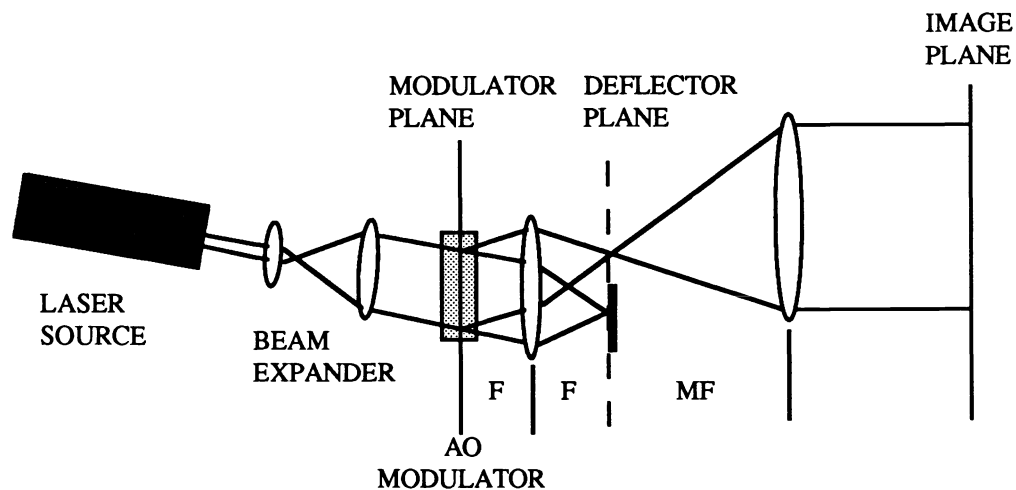


Figure 2. Scophony Process. Collimated light exposing the acousto-optic modulator is diffracted relative to the amplitude of the instantaneous video signal encountered. The acousto-optic window is Fourier Transformed at the deflector plane and reimaged at the image plane.

By choosing  $V_{\text{scan}}$  equal and opposite of  $MV_{\text{sound}}$ , we offset the motions and freeze the image in space<sup>3</sup>. To accomplish this we set

$$M = -V_{\text{scan}}/V_{\text{sound}} \quad (2)$$

and the focal length of the lens between the deflector plane and the image plane will be  $MF$ . The lens(es) between the acousto-optic and the deflector are also configured such that the acousto-optic modulator and the deflector planes are Fourier Transform planes of each other. Frequency information in the acousto-optic plane will scale through the Fourier Transform operation to position in the deflector plane. This causes the finite extent of the deflector to act as a low pass filter of the video frequency information<sup>3</sup>.

In an actual Scophony scene projector a vertical scanner is also incorporated. The 2-D image is projected into the image plane for use by system under test. Figure 3 is a diagram for the specific projector available at CREOL. Other systems may differ from this layout but the scophony process discussed above must functionally remain unchanged.

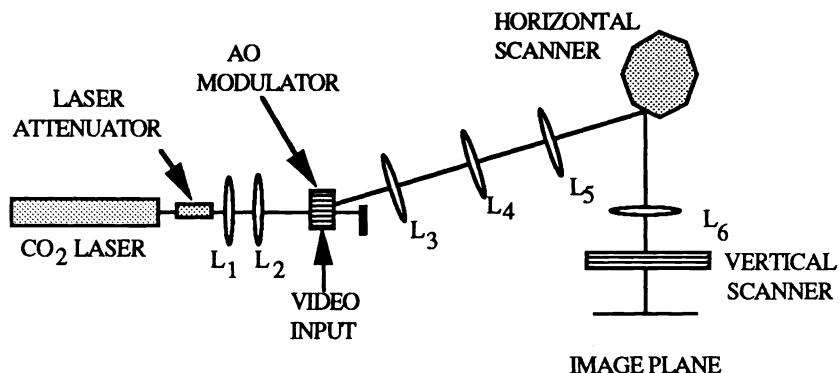


Figure 3. Scophony Scene Projector Test Configuration

### 3. SYSTEM MODULATION TRANSFER FUNCTION

The MTF of this system can be expressed as the convolution of the response of each of the constituent parts of the system. These constituents may be Fourier Transformed and multiplied to arrive at the theoretical MTF of the system. The system elements being tested here consist of the scene projector, Mercury Cadmium Telluride (MCT) detector, and a signal amplifier. Each of these subsystems will be examined to determine the expected performance.

#### 3.1 Scophony scanner MTF

The input laser energy profile to the acousto-optic modulator was measured and shown to be a gaussian energy distribution. The output of the acousto-optic cell will be the input laser energy profile coupled through Bragg diffraction with the acoustic signal.

For this experiment a sine wave generator was used in place of a video input to allow pure sinusoids to be tested. The output of the acousto-optic interaction is optically Fourier Transformed at the deflector plane and will resemble the original input laser beam gaussian profile but at the carrier frequency of the sinusoid. Frequency components of the video signal are scaled into spatial components at the deflector mirror plane by

$$y = \frac{\lambda F f_v}{V_{\text{sound}}} \quad (3)$$

As frequency is increased, the spatial position (y) also increases. For higher frequencies the gaussian profile actually falls off the edge of the scan mirror as shown in figure 4. Therefore, the limiting aperture of the deflector mirror acts as a low pass filter. For a beam centered on the deflector mirror of width A we see that

$$f_{\text{edge}} = \frac{A V_{\text{sound}}}{2 \lambda F} \quad (4)$$

The size of the mirror used in this experiment was 6.756 mm, F is 652.25 mm and  $f_{\text{edge}}$  is determined to be 2.7 MHz for an ideal Scophony scanner. Repositioning the mirror, allows one of the sidebands to fall off the edge of the mirror but also double the useful mirror surface for the other sideband<sup>4</sup>. This drives  $f_{\text{edge}}$  out to 5.4 MHz. The theoretical MTF of the scanner is shown in figure 5.

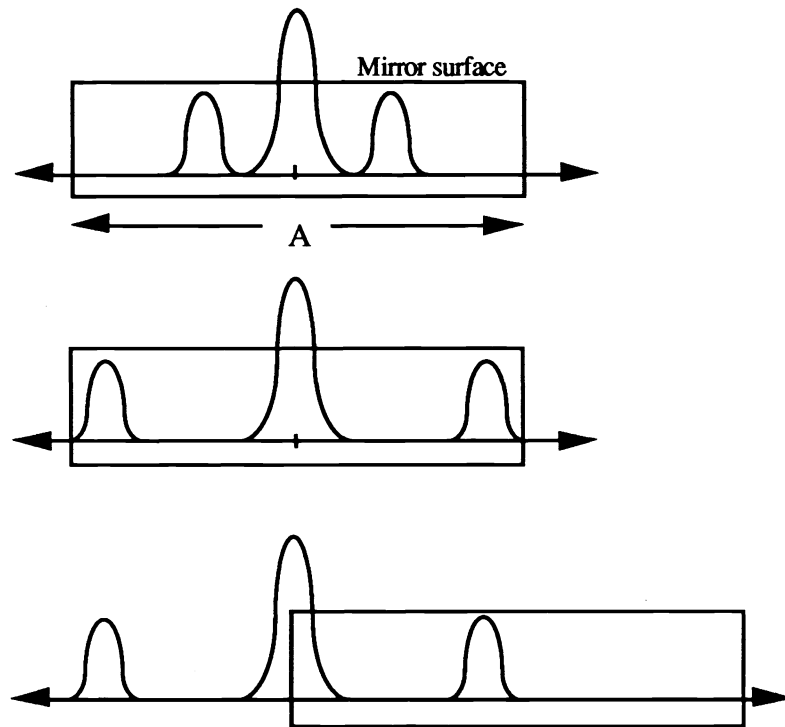


Figure 4. Frequency components translate into position at mirror surface. Frequencies beyond edge of mirror are lost. Repositioning beam doubles bandpass.

### 3.2 Detector and amplifier transfer function

The detector incorporates a 100  $\mu\text{m}$  slit to limit illumination time. The physical dimensions of the slit will cause the laser illumination to be sampled with a rectangular aperture function. The Fourier Transform of a rect function is a sinc function with units of cycle per second. The width of the rect function is a function of  $V_{\text{scan}}$  and can be readily calculated. The detector was positioned 647 mm from the horizontal scanner. This corresponds to a scan velocity of 5462 meters per second. The period of laser illumination and therefore the width of the time rect function is 18.3 nanoseconds. The theoretical transfer function of the detector is a sinc function with its first zero at 54 MHz. A plot of the frequencies of interest is shown in figure 6.

The amplifier transfer function was measured out to 6 MHz and is presented in figure 7. The amplifier -3 dB cutoff frequency was measured to be 7 MHz. Figure 8 is the expected transfer function of the Scophony system as measured through the MCT detector and the amplifier.

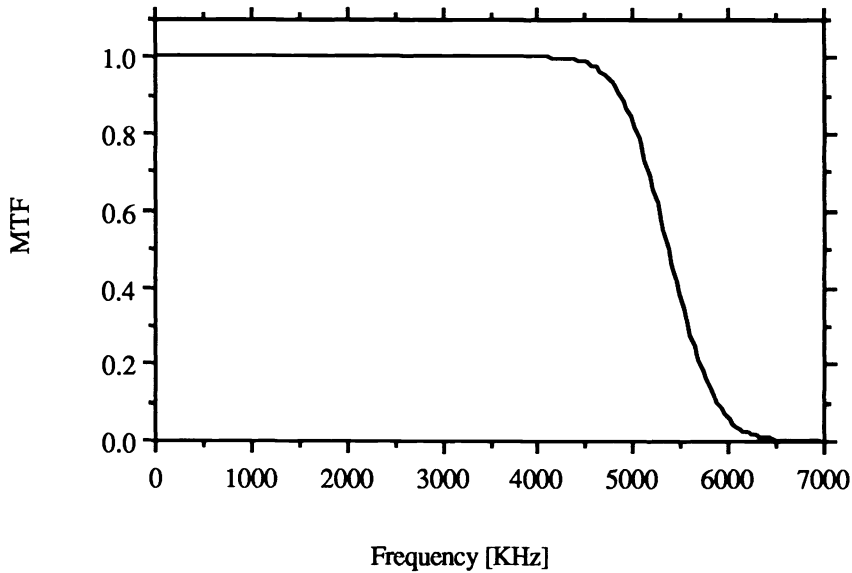


Figure 5. Theoretical MTF of the Scophony Scanner

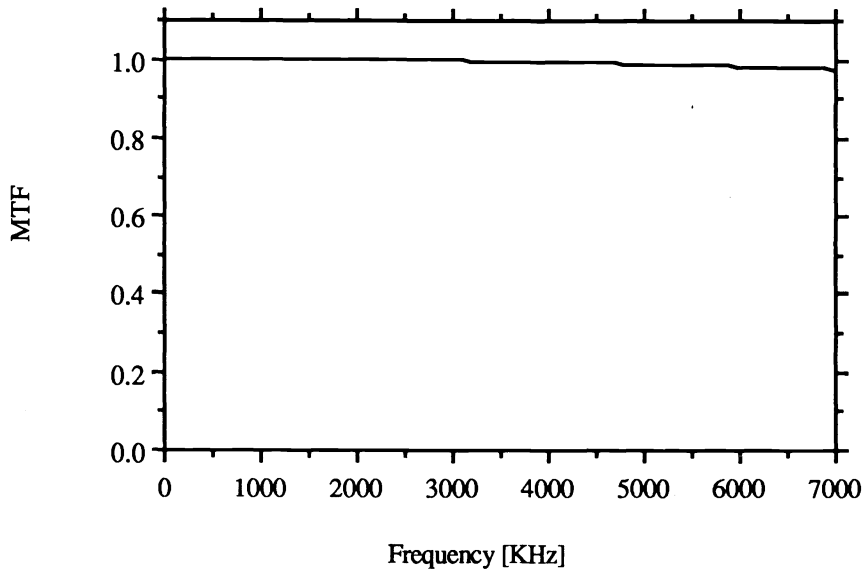


Figure 6. Calculated Detector Transfer Function

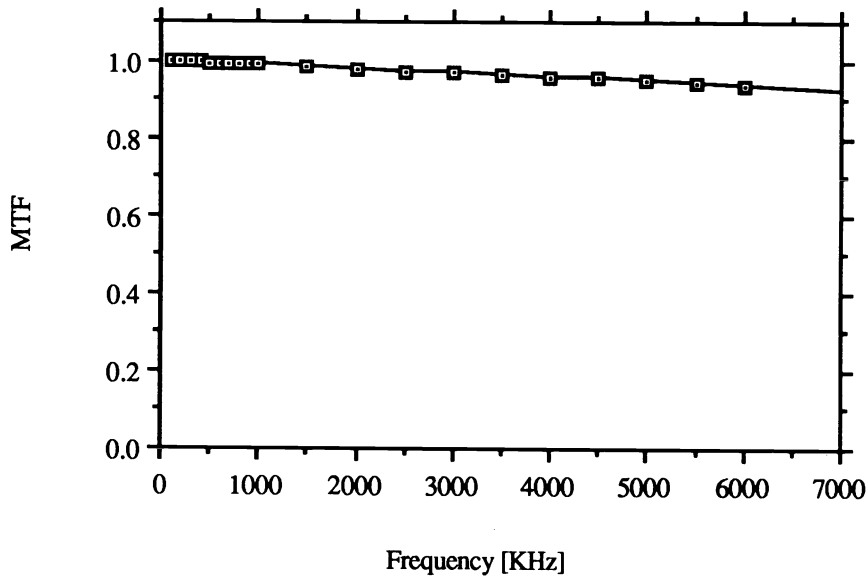


Figure 7. Measured Amplifier Transfer Function

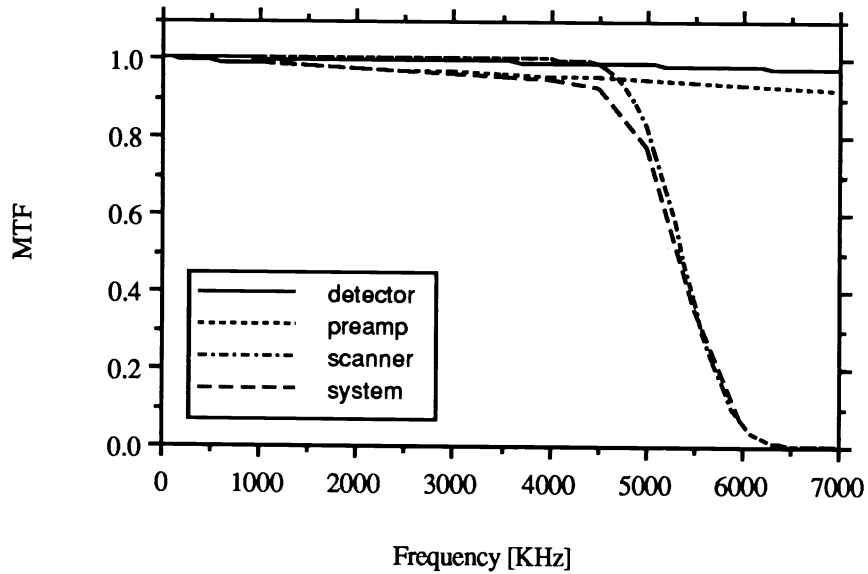


Figure 8. Summary of Expected Transfer Functions

### 3.3 MTF measurement.

Single frequency sinusoids were fed into the acousto-optic modulator using an 11 MHz signal generator. The corresponding IR output signal was measured with the MCT detector. The maximum and minimum of the output signal was measured at each frequency and used to determine the modulation depth. Figure 9 shows the measured system modulation depth vs. frequency and includes the expected system performance. As can be seen from the figure, the measured and expected MTF differ significantly.

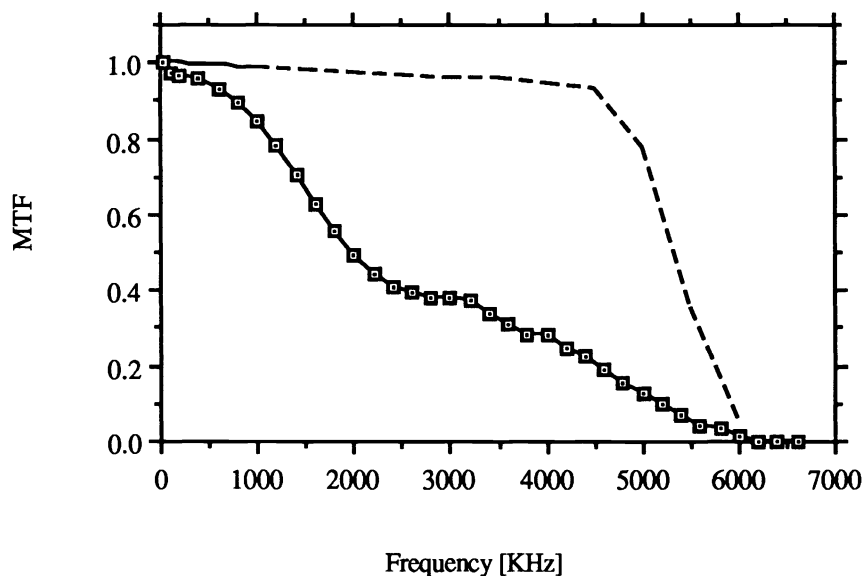


Figure 9. Measured and Expected Transfer Function

#### 4. DISCUSSION

In order to offer an explanation for the poor MTF performance, we must go back to our assumptions of acousto-optical interaction. First we will look at the nature of the input drive signal followed by an examination of the acoustic interaction.

Figure 10 shows graphically what takes place when we convolve the input sinusoid with the modulation carrier frequency. The acoustic frequency will contain elements above and below the carrier frequency. The Bragg angle has been calculated specifically for a 40 MHz signal and the hardware was positioned for maximum DC throughput. At higher input frequencies the Bragg angle shifts slightly due to the higher frequency component.

As the input beam deviates from the Bragg angle, or more correctly, as the Bragg angle deviates from the input beam, a decrease in the light coupling occurs. This decrease has been shown to vary as

$$\frac{P(\Psi)}{P(0)} = \text{sinc}^2 \left[ \frac{\pi L \Psi f_a}{v} \right] \quad (5)$$

where  $\Psi$  is the error angle

$$\Psi = \Theta_{B \text{ true}} - \Theta_{B \text{ dc}} \quad (6)$$

and  $L$  is the width of the acoustic field which has been assumed to be uniform across the acousto-optic crystal width<sup>1</sup>. The true Bragg angle at any frequency

$$\Theta_{B \text{ true}} = \arcsin \left[ \frac{\lambda (f_c + f_{in})}{2 v} \right] \quad (7)$$

will be shifted slightly from the dc Bragg angle. The Bragg angle for a dc input and 40 MHz carrier is 38.5 mrad. The Bragg angle for a 4 MHz input and a 40 MHz carrier is calculated for an acoustic frequency of 44 MHz to be 42.36 mrad. The corresponding throughput of the Scophony acousto-optic modulator is plotted in figure 11.

Incorporating this effect into the MTF predictions results in good agreement with measurement, as shown in figure 12. There is still a variation in the MTF. This is believed to be due to a nonlinearity found in the specific acousto-optic

modulator used in this experiment. Laser input and output (+1 diffraction lobe) of the modulator for a DC signal is shown in figure 13. Another potential culprit to the deviation is the validity of the assumption of a uniform acoustic wave in the modulator. Cohen and Gordon<sup>5</sup> show in the general case that the diffraction efficiency varies directly as the Fourier Transform of the amplitude distribution of the acoustic wave. Neither of these potentially degrading influences has been quantified to date.

The Bragg angle effect shown to cause degradation in the Scopphony scene projector will not readily be evident in a flying spot scanner due to the nature of the input laser beam. In the Scopphony scanner the input beam is collimated. All light is entering the modulator at the same angle. In the flying spot scanner configuration, the laser is focussed into the modulator. The focussed beam enters the modulator at all angles within the numerical aperture of the focussing optics. This compensates for the variation in Bragg angle.

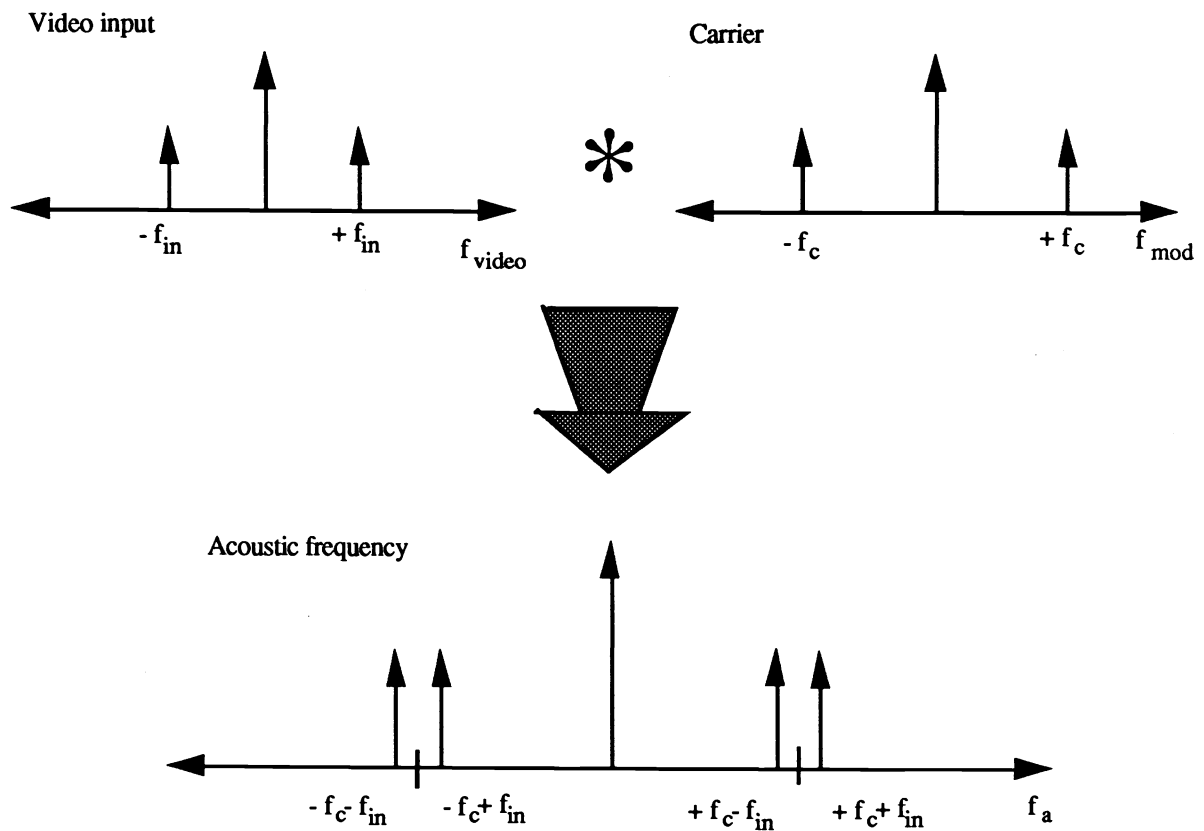


Figure 10. Convolution of input and carrier signals determine acoustic frequency and therefore Bragg Angle.



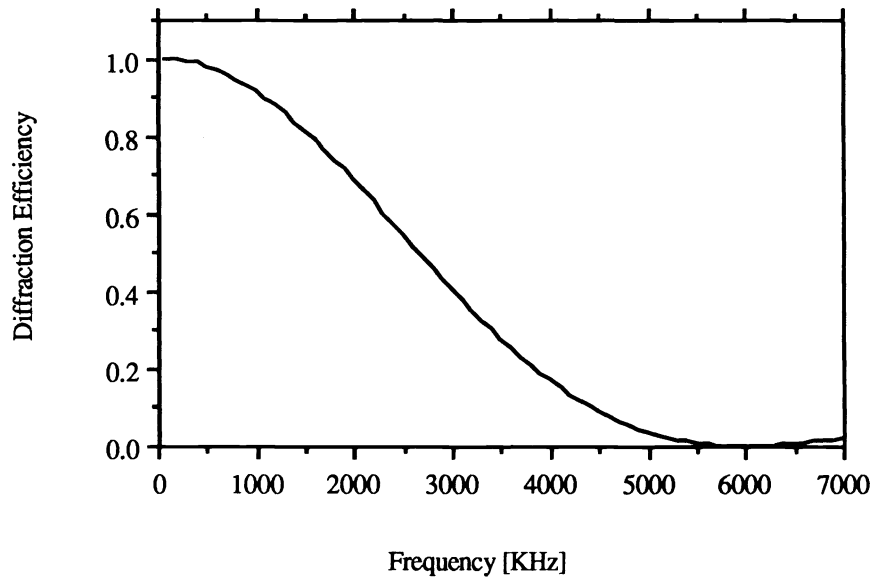


Figure 11. Variation in Diffraction efficiency due to variation in the Bragg Angle.

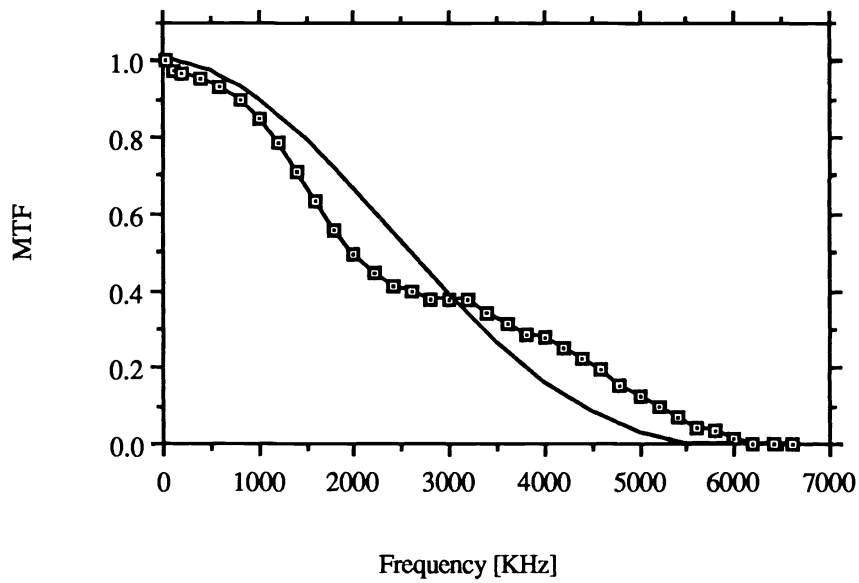


Figure 12. Measured MTF versus evaluated MTF including Bragg variation.

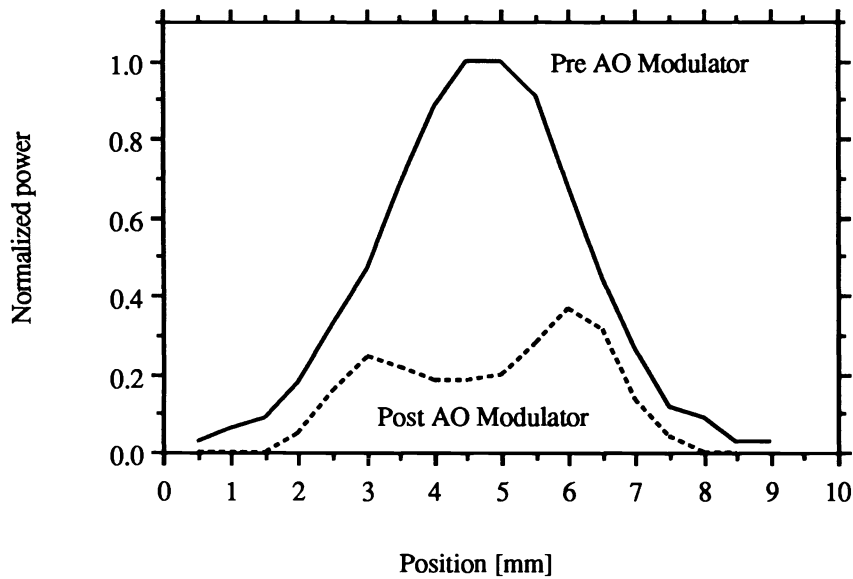


Figure 13. Normalized pre and post acousto-optic modulator laser beam profiles.

## 5. REFERENCES

1. A. Korpel, R. Adler, P. Desmares, and W. Watson, "A Television Display Using Acoustic Deflection and Modulation of Coherent Light," *Proceedings of the IEEE*, Vol 54, No.10, pp. 1429-1437, October 1966.
2. D.M. Robinson, "The Supersonic Light Control and Its Application to Television With Special Reference to the Scophony Television Receiver," *Proceedings of the IRE*, pp. 483-486, August 1939.
3. R. V. Johnson, "Scophony Light Valve." *Applied Optics* Vol 18, No. 23, pp. 4030-4038 December 1979.
4. R. V. Johnson, J. Guerin, and M. E. Swansberg, "Scophony Spatial Light Modulator" *Optical Engineering*, Vol 24, No. 1, pp. 83-100. January/February 1985.
5. M. G. Cohen and E. J. Gordon, "Acoustic Beam Probing Using Optical Techniques," *The Bell System Technical Journal*, pp. 693-721, April 1965.

This work was partially supported by the Florida High Technology and Industry Council.